Egyptian Journal of Agricultural Research

Efficacy of PCR-bassed techniqes and remote sensing technology for detecting potato brown rot infection caused by *R. solanacearum*

*Naglaa Mousa Balabel [1' 2], Mamdouh M. Ali [3], Shams Nour El-Dein Younes [4]

[1] Plant Pathology Research Institute, Agricultural Research Center (ARC), Giza, Egypt.

[2] Potato Brown Rot Project (PBRP), Ministry of Agriculture and Land Reclamation, Dokki, Egypt.

[3] Geology Department, Faculty of Science, Al-Azhar University, Nasr City, Cairo, Egypt.

[4] Department of Geography, Faculty of Arts, Cairo University, Giza, Egypt.

*Corresponding author: Naglaa M. Balabel. nbalabel@yahoo.com

Abstract

Bacterial wilt of potatoes (Solanum tuberosum) caused by Ralstonia solanacearum phylotype II sequevar I (race 3 biovar 2), is one of the most serious diseases of potatoes. This study aimed to detect such deteriorations through the remotely sensed data. In this regard, naturally infested potato fields at Abo Alkhawi, Al Tayareya and Om Saber villages at Behera governorate, Egypt, were used for selective isolation of R. solanacearum. On Semi Selective South Africa (SMSA) medium, 30 isolates were randomly screened and tested by immunofluorescence antibody staining (IFAS) and confirmed biologically by tomato plantlets (cv. Pinto) reaction. All isolates showed positive results with Real-time PCR. Based on the phylotype specific multiplex (Pmx) – PCR data, all isolates in concern were R. solanacearum and affiliated to phylotype II as 372- bp amplicon.

Spectral indices were applied on the Landsat 8 and RapidEye satellite images acquired in January and April 2019 including Normalized Difference Moisture Index (NDMI), Normalized Difference Vegetation Index (NDVI), Normalized Difference Salinity Index (NDSI) and Modified Chlorophyll Absorption Ratio Index (MCARI). Results from the remote sensing analyses showed medium to relatively high salinity and moisture content of soils concerened. Moreover, plants chlorophyll levels are in medium levels which is not typical to condition associated with usual circumstances. Further investigation, in a greater academic depth, are needed for pathological field surveys.

Keywords: SMSA medium, immunofluorescent antibody staining (IFAS), Phylotype analysis, Real-time PCR, wilt and brown rot diseases, indices, Landsat 8, RapidEye, soil salinity, moisture content and chlorophyll content.

Plant Patholog

Introduction

El Beheira governorate is one of the largest governorates of Egypt in the cultivation and production of potatoes, where, its total cultivated area of potatoes reaches 69768 fedden out of a total of 251508. While its production of potato crop reaches 793404 ton out of a total of 2915342 (Economic Affairs Sector, 2018). For this reason, precautionary determinations should be taken while planting such strategic crop by using the modern lab determinations and the possible remote sensing technologies to detect potato infection with brown rot disease caused by *R. solanacearum.*

R. solanacearum pathogen is soil and tuber- borne bacterium (Kabeil *et al*., 2008), which causes bacterial wilt disease of potatoes or potato brown rot. Accordingly, it is a serious disease of potatoes and many other cultivated plants (Hayward & Hartman, 1994). This pathogen causes wilt syndrome for more than 450 plant species belonging to 54 different botanicals families (Caitilyn *et al*., 2005). The pathogen invades the plant through the points of root emergence and rapid multiplication leading to brownish discoloration and collapse of the vascular tissue (Hayward, 1991). Symptoms associated with infected plants are wilting, stunting and yellowing of the foliage (Kelman, 1953). The rate of disease development is depending on host susceptibility and the aggressiveness of the pathogenic strain.

In potato tubers the internal symptoms of the disease display a greyish-brown discoloration of vascular elements and milky-white sticky bacterial ooze is seeping out while in severe infection it may be visible at tuber eyes or at the stolon end scar. In some cases, these tuber symptoms are visibly absent and be as a latent infections.

Disease transmission may be through contaminated farm tools and equipments, latently infected planting material, plant debris, contaminated irrigation water, some weeds, insects, deep wounding during cultivation and nematodes. Moreover, this bacterium can move from the roots of infected plants to adjacent roots of healthy plants, as root to root infection (Ji *et al*., 2005).

R. solanacearum can survive long-term in soil under natural conditions because of a lack of sensitive detection methods for studying low pathogen populations amongst high numbers of saprophytic bacteria in the soil environment. Standard methods to monitor the present of pathogen in potato tubers include using of immunofluorescence antibody staining (IFAS), isolation on selective medium such as (SMSA) medium (OEPP/EPPO, 1990). While the most commonly used techniques to confirm positive results in IFAS test are the bioassay on tomato

plants (as indicator plant). Also, using polymerase chain reaction (PCR) from pure single colony that has been isolated from selective medium (OEPP/EPPO, 1990).

Many studies and trials have been carried out worldwide to control this serious disease through farming practices but without much success. Although crop rotation with non-host plants was recommended but had proven as inefficient method. While, using soil fumigants is environmentally unacceptable, expensive and largely ineffective against the disease (Saddler, 2005). The same conclusion was reached with antibiotics and chemical control (Murakoshi and Takaha shi 1984, and Habashy *et al.*, 1993) while, breeding of new resistant varieties is consider a new stratiegy for controlling the disease (Lo´pez and Biosca 2004). As the outcome of failure and difficulties of control, the early detection of the disease is highly desired as preliminary aspects of management. Chiwaki *et al*. (2005) mentioned that using thermal infrared imagery induced a decrease in photosynthesis, transpiration and stomatal conductance which are closely related to the increase in plant leaf temperature. So, they depend on this method to detect the infection 4 days earlier to the appearance of visual diagenostic symptoms where, the invasion of vascular bundles and bacterial multiplication were lowering transpiration and raising leaf temperature. Also, remote sensing technique and image analysis allows the early detection of any morphological and anatomical changes even if these changes are small, without any physical contact between the measuring device and the studied object. Moreover, the object can be analyzed many times noninvasively and without damage (Nilsson, 1995 and Cha´vez *et al*. 2009, 2010).

As the remarkable attractive symptom of infection being the decrease in the chlorophyll content resulted from wilting and yellowing change on foliage and the fact that remote sensing technique may accurately detect those changes. The current study aimed to monitor and detect such symptoms changes through the remotely sensed data obtained from satellite images. For this purpose, satellite images obtained from Landsat-8 – Operational Land Imager (OLI) and RapidEye were used to detect the presence of wilting conditions on potato plant at wider scale and confirmatory detection.

Material and Methods:

The data and methodology of the current study are simply displayed in Figure (1), where they included two main parts, A) Fieldwork and lab analyses, B) Remote Sensing Analyses.
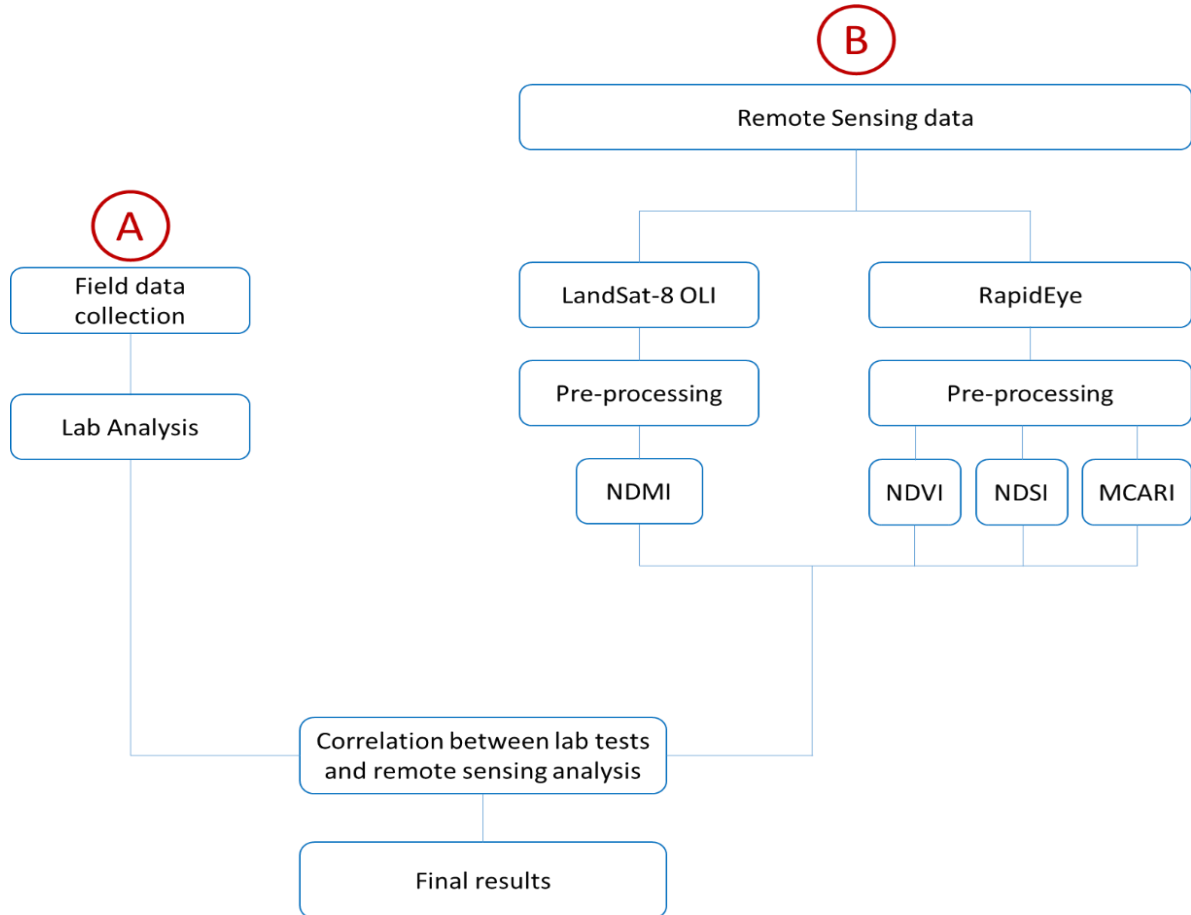
Figure, 1: Simplified flowchart for the adopted methodology,
    A) Fieldwork and lab analyse
    B) Remote Sensing Analyses

A. Fieldwork and lab analysis

1. Study area location:

Three Egyptian villages *i.e.,* Al Tayreya, Abo Al Khawi, and Om Saber belonging to El Beheira governorate, which lied in Nile North Delta were selected as work area of this investigation (Figure, 2). This area is characterized by relatively high temperature in the summer and warm conditions in the winter, where, the highest temperature in the summer

reaches about 32.1°C in July, while the lowest temperature in the winter reaches about 7.6°C in January (Egyptian Ministry of Environment, 2007).

Soil samples were collected from three selected areas of investigation and examined for the presence of *R. solanacearum* bacterium that cause potato brown rot infection. Sixteen samples from each field were taken at approximately 20 cm depth, using a sampling auger, mixed well and sieved through 2.0 mm mesh size in the laboratory for homogenization. For the microbiological analyses the tested sample was splitted into (4) fractions.

2.   Isolation of Ralstonia solanacearum:

Isolation from soil was made on SMSA as selective medium for the pathogen (Elphinstone *et al*., 1996). Decimal dilutions of the original suspension were made in 90 mL sterile phosphate buffer (0.05 M), then they were shaked for 2 hours at 15°C and plated onto SMSA medium. The plates were incubated at 28°C for few days (almost 5 days).

The typical isolates which appeared as fluidal, slightly irregular, white colonies with pink centers were selected (Buddenhagen & Kelman, 1964). Thirty isolates were randomly selected and cultured on nutrient agar medium for 48 hours, and then they were verified serologically using IFAS test (Janse, 1988). The selected isolates were kept as suspensions in sterile tap water for long-term storage as bench incubation then they were revived by culturing on tetrazolium chloride (TTC) medium (Kelman, 1954), when being desired.

1. Biovar determination of the pathogen:

Biovar characterization of the bacterium was done according to its ability to oxidize sugar and sugar alcohols as described by the standard procedure of Hayward, (1964).

2. Pathogenic potential of isolates:

Pathogenicity of randomly selected isolates recovered from different area of investigation were biologically confirmed by inoculating tomato (*Solanum lycopersicum* cv. Pinto) plantlets (3 leaves/ seedling), grown in pots under greenhouse conditions, using the stem puncture technique (Janse, 1988). Injection was made at the leaf axis by a needle laden with the bacterial growth of the pathogen. Few drops of sterile water were injected instead of bacteria as a control treatment. The inoculated plants were covered with polyethylene bags for one day, kept at 30°C, then, the bags were removed, and pots were irrigated and examined for wilting symptoms.
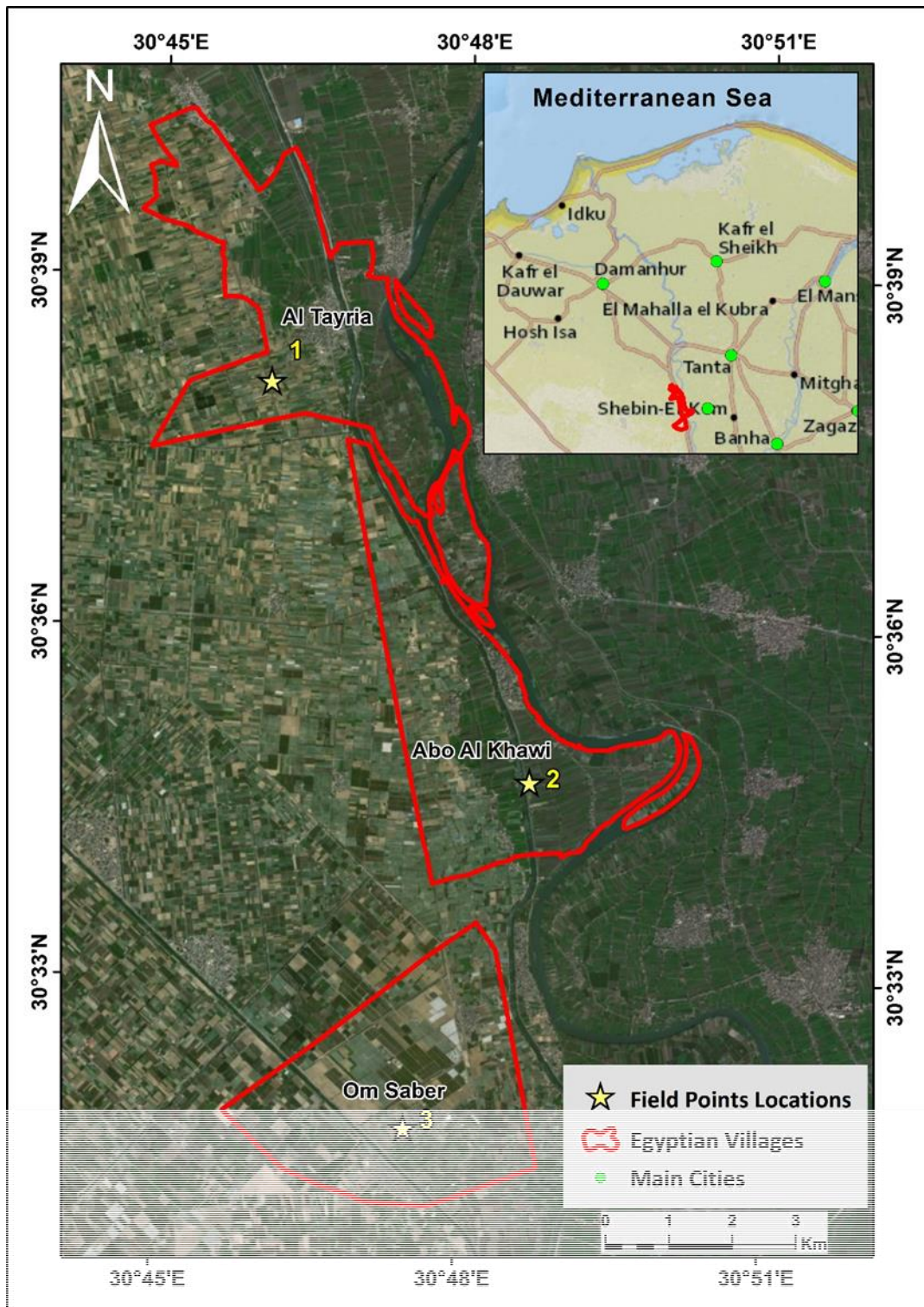
Figure, 2: RapidEye image (bands 3, 2, 1) showing the location of the study area at El   Beheira Governorate, Egypt.

3.   **Real-time PCR assay:**

Real-time PCR (Taq-Man) for DNA amplification was preformed as described by Weller *et al.* (2000) using Applied Biosystem7500 real-time machine. All selected isolates from different soils were tested by this technique. The reaction mixture consistes of: 12.5µl of master mix, 1.0 µl of primer forward, 1.0 µl of primer reverse, 1.0 µl of probe and 7.0 µl of water and 2.5µl of nucleic acid extract. The sequence of used primers and probe is shown in Table (1) and were provided by OPRON, USA. Positive control of extracted DNA was used while, the water was used as a negative control.

Table (1) : Sequence of primers and the Taq-Man probe used to detect R. solanacearum by Real-time PCR.

Primer or probe name	Primer or probe sequence(5'→3')	Length	Dye
RS-I-F	GCA TGC CTT ACA CAT GCA AGTC	22	
RS-II-R	GGC ACG TTC CGA TGT ATT ACT CA	23	
RS-P	AGC TTG CTA CCT GCC GGC GAG TG	23	FAM

4.   **Phylotype analysis of R. solanacearum by Multiplex- PCR**

Phylotype analysis of selected *R. solanacearum* isolates was made by using the Opina primers 759/760 as internal markers which is specific for the *R. solanacearum* species and a set of 4 phylotypes-specific forward primers with a unique and conserved reverse primer targeted in the 16S-23S Intergenic Spacer region (Opina *et al.*, 1997). Table (2) shows the sequences of these primers. One colony is suspended in 100.0µl of sterile water and is heated for 5 minutes at 100°C and the debris are spined down. The reaction mixture consists of: 12.5µl of ready master mix, 1.0 µl from each primer, 3.5µl of water and 2.0µl of nucleic acid extract (Sagar *et al.*, 2014).

The cycling program was used in a thermal cycler (Biometra T personal) as following: 96°C for 5 min and followed by 30 cycles of 94°C for 15s, 59°C for 30s and 72°C for 30s, then followed by a final extension period of 10 min at 72°C. A 13.0µl aliquot of each amplified PCR product was subjected to electrophoresis on 2% (w/v) agarose gels, contains ethidium bromide (0.5% µgL-1) and then the bands were visualized on a UV- transilluminator. The Pmx-PCR test amplifies the 280-bp universal *R. solanacearum* specific reference band plus following phylotype-specific PCR products: a 144-bp amplicon from phylotype I strain; a 372-

bp amplicon from phylotype II strains; a 91-bp amplicon from phylotypeIII strains and a 213-bp amplicon from phylotype IV strains (Sagar *et al.*,2014).

Table (2): Sequence of primer bases used for phylotype determination of R.solanacearum by Multiplex PCR.

Primer name	Primer Sequence (5` →3`)	Length
759	GTC GCC GTC AAC TCA CTT TCC	21
760	GTC GCC GTC AGC AAT GCG GAA TCG	24
Nmult:21:1F	CGT TGA TGA GGC GCG CAA TTT	21
Nmult:21:2F	AAG TTA TGG ACG GTG GAA GTC	21
Nmult:23: AF	ATT ACS AGA GCA ATC GAA AGA TT	23
Nmult:22: IMF	ATT GCC AAG ACG AGA GAA GTA	21
Nmult:22: RR	TCG CTT GAC CCT ATA ACG AGT A	22

B. Remote Sensing Analysis

Different satellite images with different spatial and spectral resolutions were used with Landsat 8- Operational Land Imager (OLI) and RapidEye sensors. United States Geological Survey (USGS) and Planet Labs websites were used to download the satatllite data. Table (3) shows that, the satellite images were downloaded on two different dates, January 2019 and April 2019, before planting of the fields and after 45 days of planting, respectively.

Table (3): Remote sensing data sources and description

Sensor	Source	No. of Scenes	Acquisition Date	Cloud Cover (%)
Landsat 8	https://earthexplorer.usgs.gov	1	20/01/2019	1.02
RapidEye (RE)	www.planet.com	2	22/01/2019	0
		2	24/04/2019	0

1. RapidEye satellite data

The RapidEye is a multispectral and high-resolution satellite that consists of a constellation of five earth imaging satellites through identical sensors that are in the same orbital plane and are calibrated equally to one another. This means an image from one RapidEye satellite will be identical in characteristics to an image from any of the other four satellites (Planet Labs 2016).

Data from RapidEye are produced as individual 25km by 25km tiles and offered in different processing levels. The sensor is having a five-channel multispectral system operating in the visible and near-infrared (Warner *et al.,* 2009) with a spatial resolution of 5 meters as shown in Table (4). Four level 3A scenes were used in the current study, 2 scenes from January and 2 others form April 2019, which are radiometrically, geometrically corrected and projected to map projection (Planet Labs, 2016). Both tiles from each date were mosaicked together and clipped to match the boundary of the study area to reduce the amount of time taken in processing.

Table (4): RapidEye satellite specifications (modified after Planet Labs, 2016)

Spectral Bands	Spectral Range (nm)
Band 1 – Blue	440 – 510
Band 2 – Green	520 – 590
Band 3 – Red	630 – 685
Band 4 - Red Edge	690 – 730
Band 5 – NIR	C. – 850

2. Landsat 8- OLI sensor

The Landsat 8 satellite is carrying two different sensors the Thermal Infrared Sensor (TIRS) and Operational Land Imager (OLI) (Roy *et al.*, 2014). The Landsat 8 two sensors providing a seasonal coverage of the world at different spatial resolutions 30m (visible, NIR, SWIR), 100m (thermal), and 15m (panchromatic) (Ennaji *et al*., 2018) as shown in Table (5).

Table (5) : Specifications of Landsat 8 satellite images, (modified after Roy et al., 2014)

Band description	Wavelength (μm)	Spatial resolution (m)
Band 1 — coastal/aerosol	0.43–0.45	30
Band 2 — blue	0.45–0.51	

Band 3 — green	0.53–0.59	
Band 4 — red	0.64–0.67	
Band 5 — near-infrared	0.85–0.88	
Band 6 — shortwave infrared	1.57–1.65	
Band 7 — shortwave infrared	2.11–2.29	
Band 8 — panchromatic	0.50–0.68	15
Band 9 — cirrus	1.36–1.38	30
Band 10 — thermal Infrared	10.60–11.19	100
Band 11 — thermal Infrared	11.50–12.51	

Only one scene from Landsat 8 was used in the date before planting, also bands from 1 to 7 were stacked together to make the image ready to apply the atmospheric corrections .The effects of the atmosphere (scattering and absorption) and the pixel values were finally converted to surface radiance, then the corrected image was clipped to match the boundary of the study area.

3. Construction of soil and vegetation indices:

Four different indices were applied to the downloaded and preprocessed satellite images in before and after planting dates including the Index (NDVI), (NDSI), (NDMI), and (MCARI).

2. Before planting indices construction

Three indices were applied to the images of RapidEye and Landsat 8 starting from the NDVI, NDSI, and NDMI. Both NDVI and NDSI were applied to the images of RapidEye, while the NDMI was applied to Landsat 8 image.

The NDVI index is used to detect the density of plants on a particular part of land (Weier & Herring, 2018). Where, it utilizes the absorptive and reflective characteristics of the vegetation in the red and near-infrared portions of the electromagnetic spectrum. Therefore, the NDVI was used in the current study and specifically on the January image (Figure, 3) to make sure that the field is bare and not vegetated which will give a great opportunity to apply and measure the soil characteristics of the land.

The NDVI calculated using the following equation:

$$NDVI = \frac{NIR - RED}{NIR + RED}$$

Where:

NIR = Near Infrared band (RapidEye, band no. 5)

RED =RED band (RapidEye, band no. 3)

The NDSI which has been proposed by (Aldakheel *et al.*, 2005) is the widely used index to extract and measure the soil salinity due to its significant correlation with Electric Conductivity (EC) (Ennaji *et al.*, 2018). The index can be calculated by using the following equation:

$$NDSI = \frac{RED - NIR}{RED + NIR}$$

Where:

NIR = Near Infra-Red band (RapidEye band no. 5)

RED =RED band (RapidEye band no. 3)

The resulted NDSI map is dimensionless and ranges between −1 (low salinity content) to +1 (high salinity content) as shown in Figure (4).

The NDMI is a measure of the amount of water in the soil which in turn reflects and estimate the moisture content of the soils (Serrano *et al*., 2019). The following equation is used to calculate the NDMI:

$$NDMI = \frac{NIR - SWIR}{NIR + SWIR}$$

Where:

NIR = Near Infra-Red band (Landsat 8 band no. 5)

SWIR =Short Wave Infra-Red band (Landsat 8 band no. 6)

As seen in the above NDMI equation the presence of the SWIR spectral band is required to run the analysis on the study area. For this reason, the Landsat 8 image was used to calculate and measure the moisture content of the soils of the study area (Figure ,5).
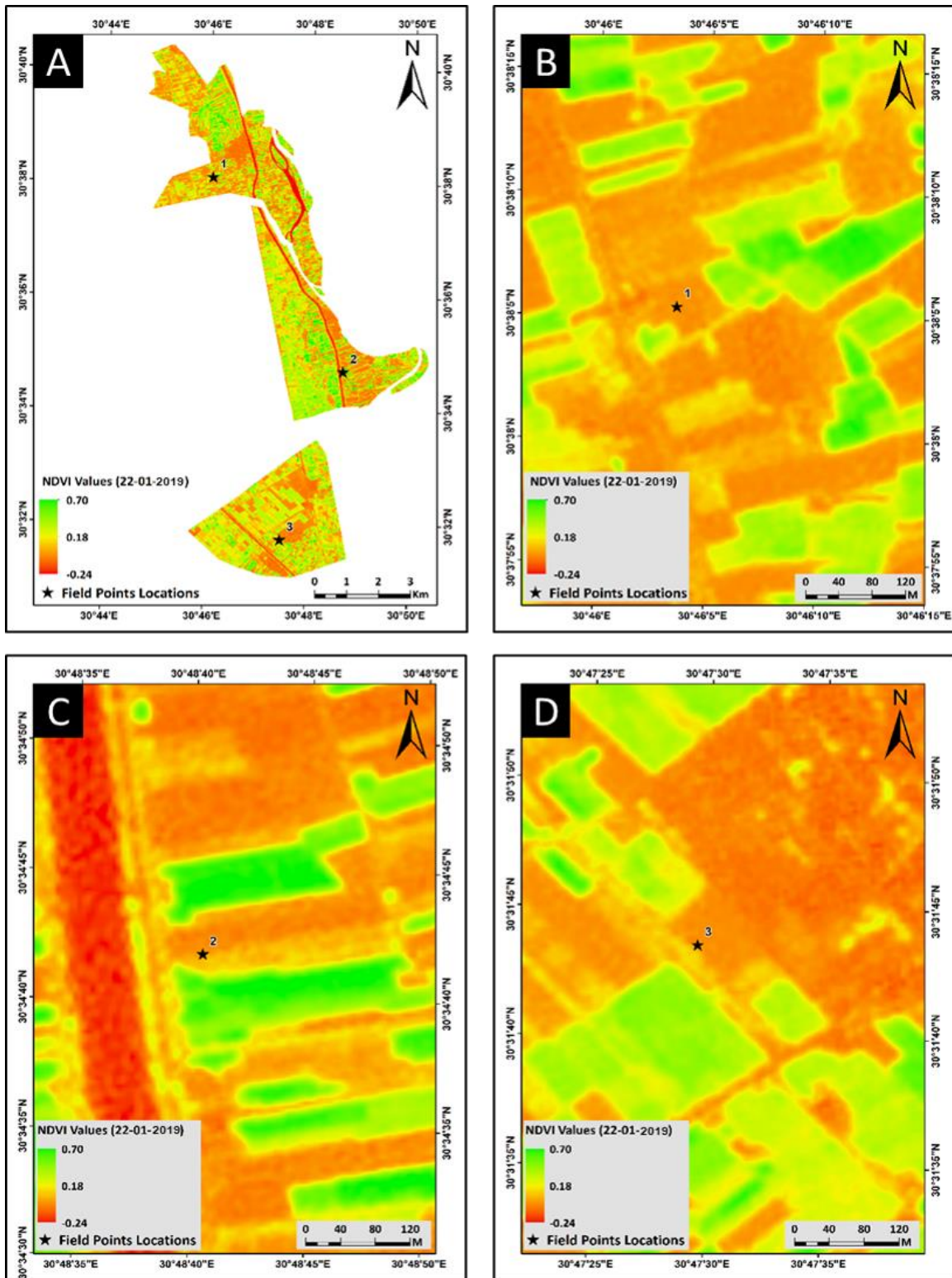
Figure, 1: A) RapidEye extracted NDVI for the whole study area before planting the field, B) Location of field point no. 1. C) Location of field point no. 2. D) Location of field point no. 3.

3. After planting indices construction

Two determinations were made (NDVI and MCARI) using the images of RapidEye. The NDVI was applied again over that date for double-checking the planting status of the field (Figure, 6).

MCARI is strongly affected and sensitive to chlorophyll concentrations in plant leaves (Xue & Su, 2017). It can be calculated using the following equation:

$$MCARI = \frac{1.5[2.5(\rho_{800} - \rho_{670}) - 1.3(\rho_{800} - \rho_{550})]}{\sqrt{(2 * \rho_{800} + 1)^2 - (6 * \rho_{800} - 5 * \sqrt{\rho_{670}}) - 0.5}}$$

Where:

ρ_{800} = NIR band (RapidEye band no. 5).

ρ_{670} = RED band (RapidEye band no. 3)

ρ_{550} = Green band (RapidEye band no. 2)
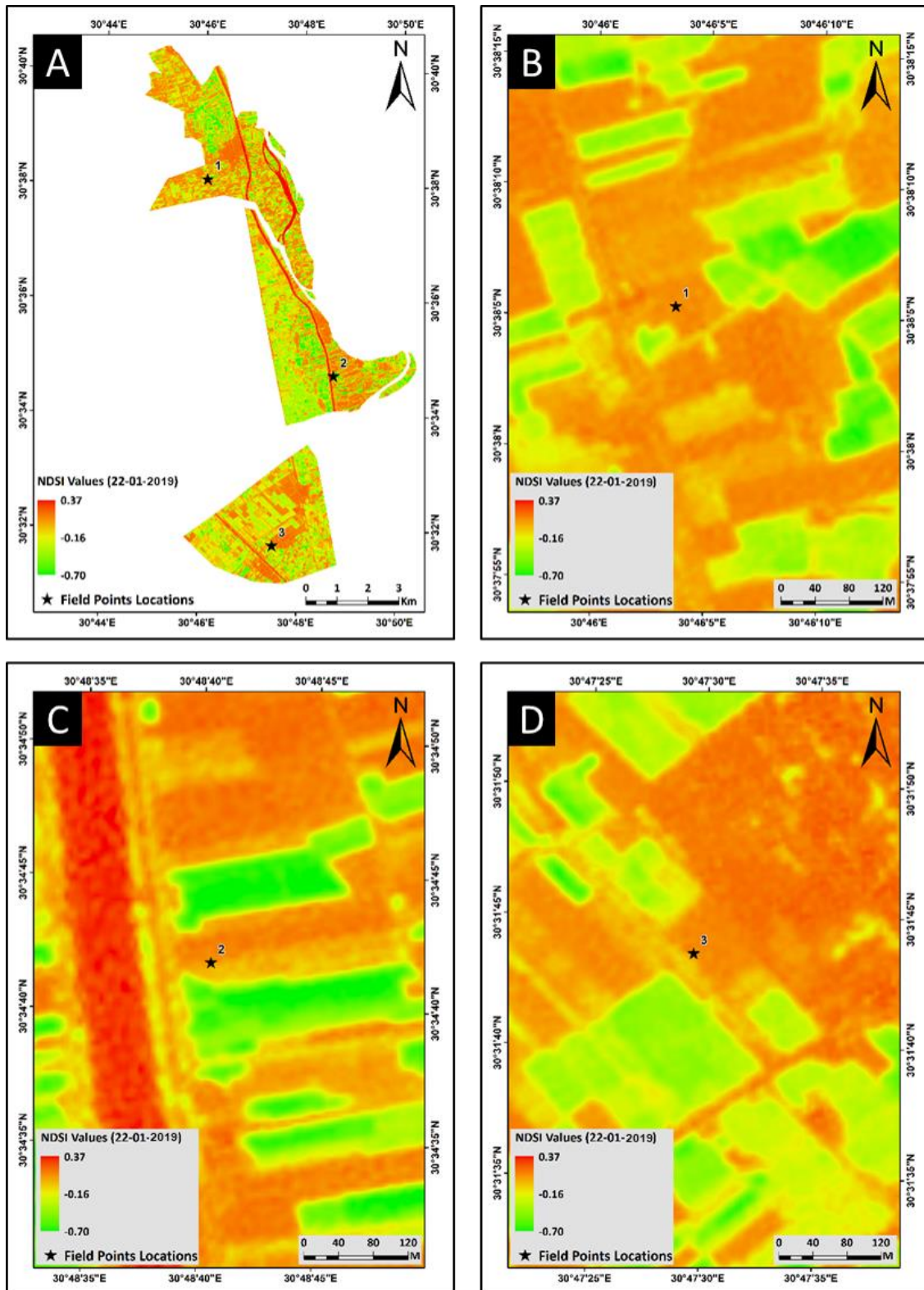
Figure, 2: A) RapidEye extracted NDSI for the whole study area before planting the field. B) Location of field point no. 1. C) Location of field point no. 2. D) Location of field point no. 3.
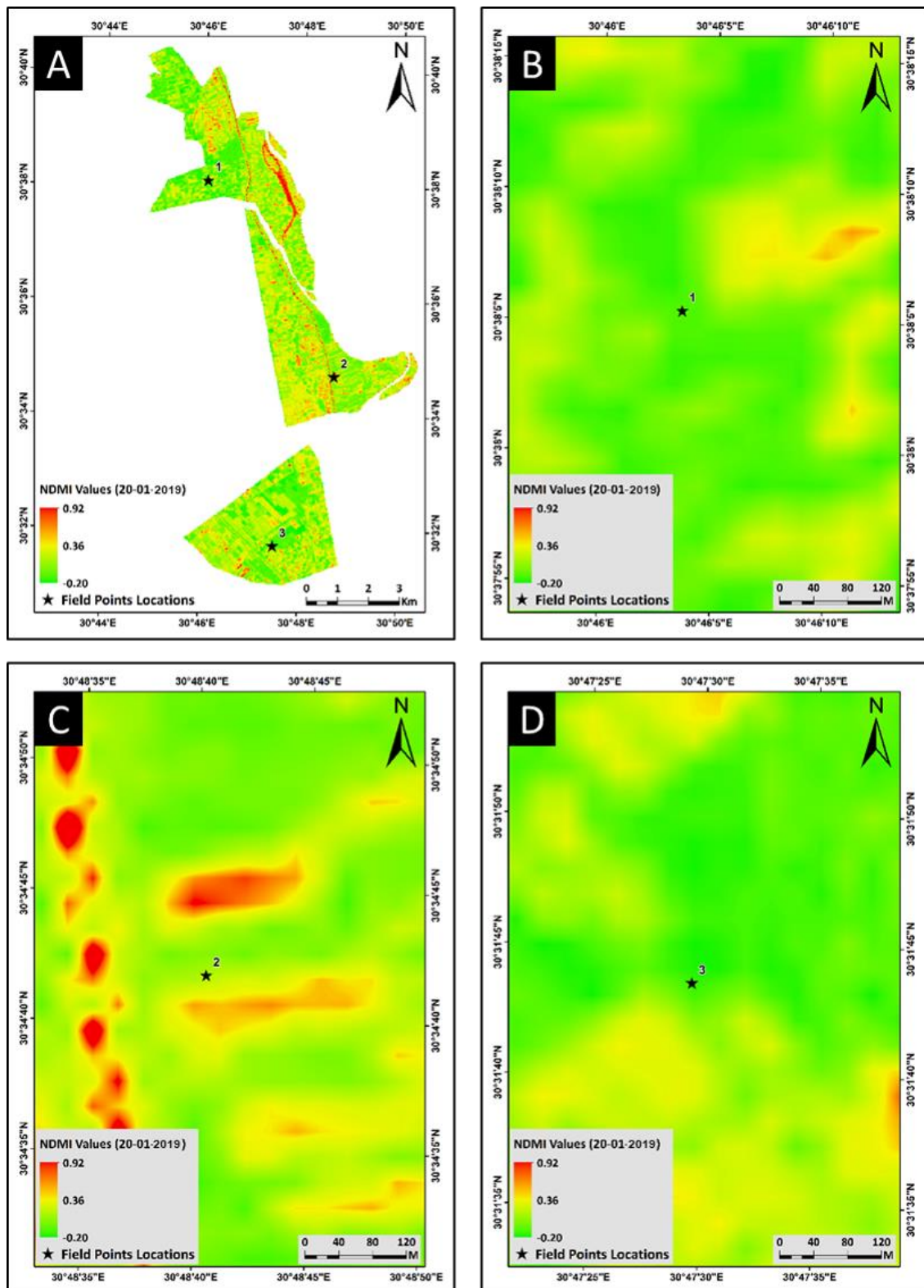
Figure, 3: A) Landsat 8 extracted NDMI for the whole study area before planting the field. B) Location of field point no. 1. C) Location of field point no. 2. D) Location of field point no. 3.
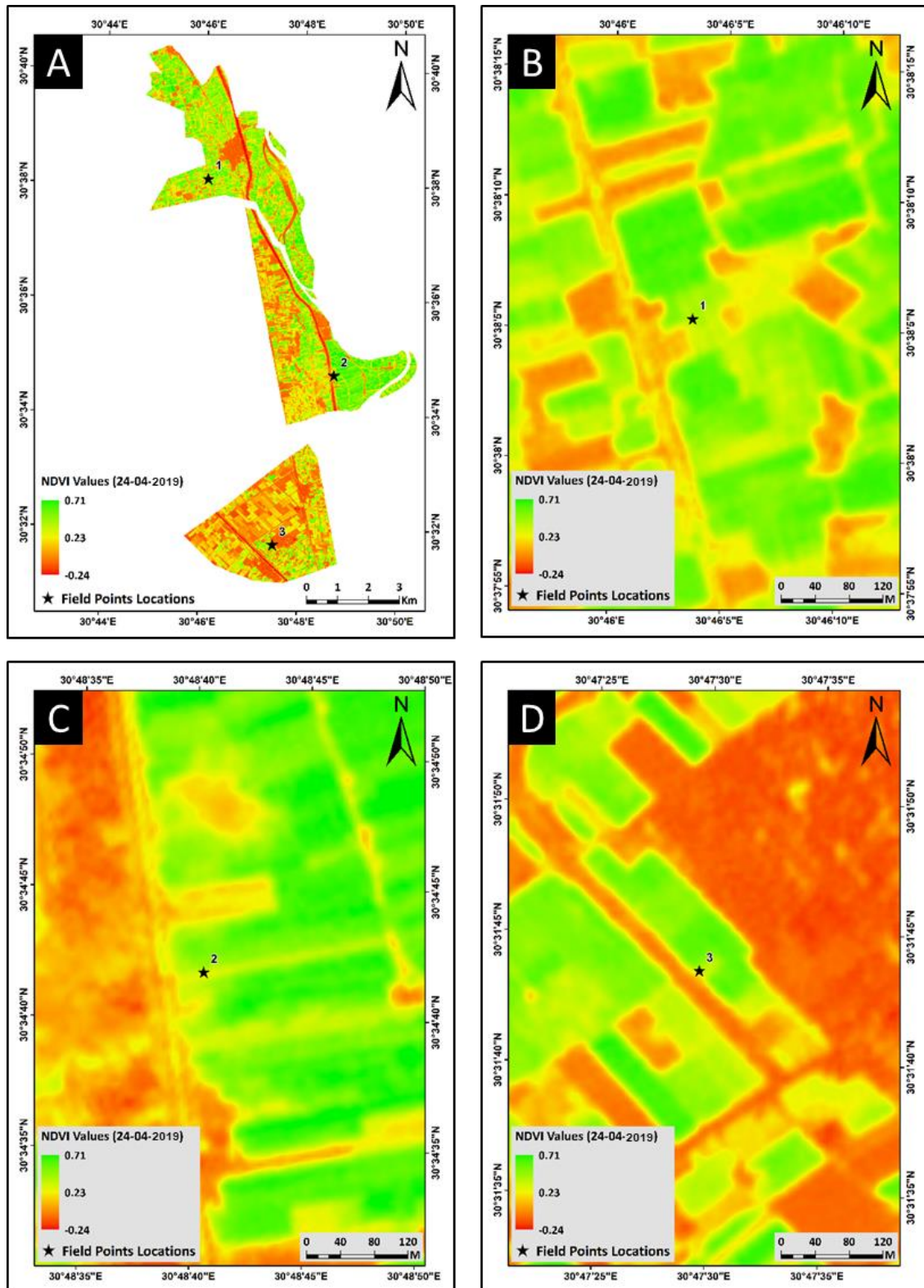
Figure, 4:   A) RapidEye extracted NDVI for the whole study area after planting the field.
B) Location of field point no. 1. C) Location of field point no. 2.
D) Location of field point no. 3.

Also, it's not affected by the illumination conditions, the background reflectance from observed soil and other non-photosynthetic materials. To this end, this index was used to measure the chlorophyll content of the potato crop leaves in the study area as shown in Figure ,(7).
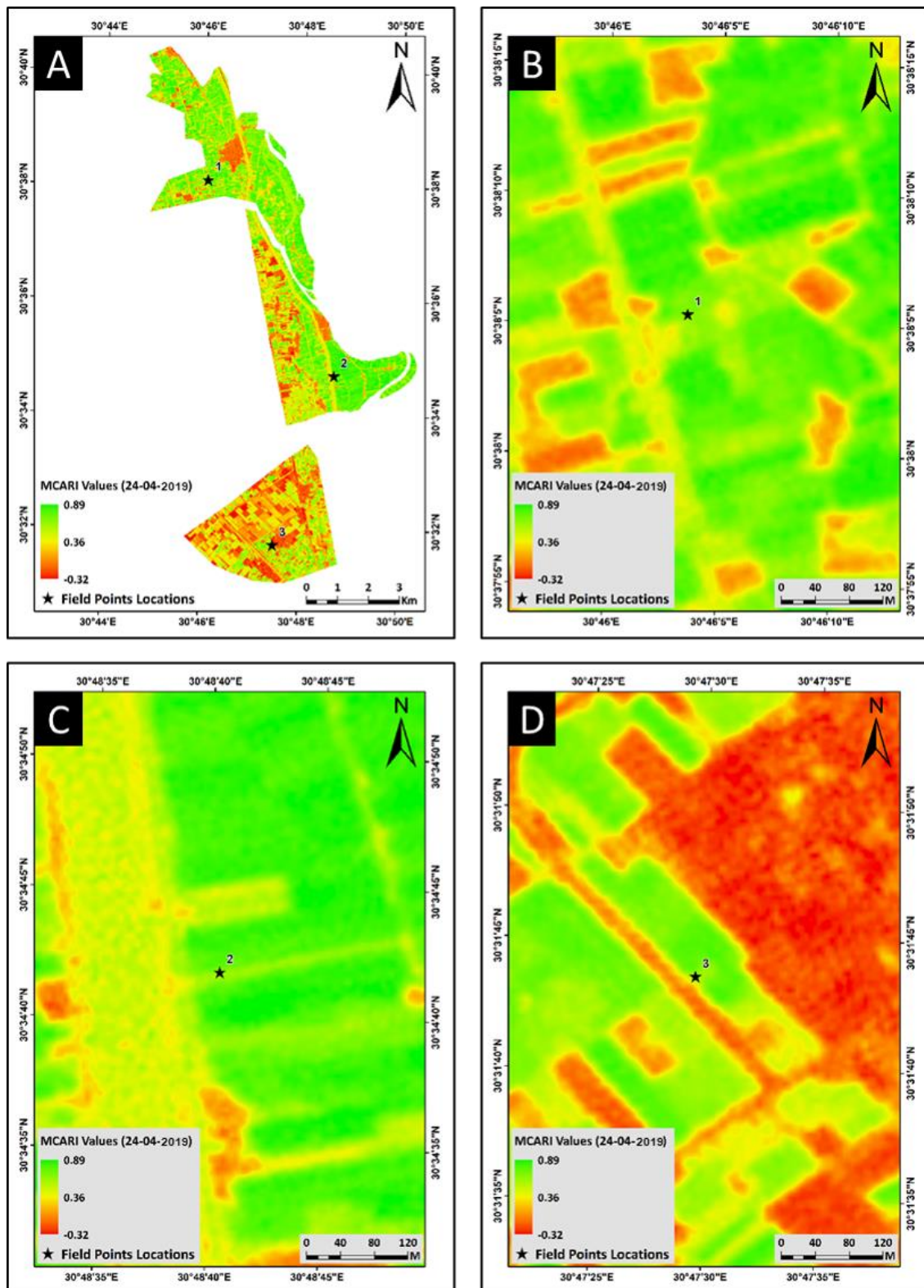
Figure, 5: A) RapidEye extracted MCARI for the whole study area after planting the field.
B) Location of field point no. 1. C) Location of field point no. 2.
D) Location of field point no. 3.

Results

1. **Isolation of *Ralstonia solanacearum* from different potato fields:**

    Naturally infested soil samples from different potato fields in villages in concern were used for isolation of *R. solanacearum* bacterium. Morphological characteristics of isolates were described on SMSA medium. On that medium, all isolates showed fluidal, milky white, irregular with blood red center was identified as typical colonies of *R. solanacearum.* The numbers of bacteria were 20 x 10^4, 31 x 10^4 and 48 x 10^4 from Al Tayreya, Om Saber and Abo Al Khawi villages respectively. Thirty isolates were randomly selected (12 isolates from Abo Al Khawi area, 9 isolates from Om Saber, as well as 9 isolates from Al Tayreya area).

2. **Immunofluorescent antibody staining test (IFAS)**

    All randomly selected colonies (thirty isolates) developed on SMSA medium were tested by IFAS test. The cells showed short rod shaped morphology, stained evenly as bright green fluorescent (Figure.,8).
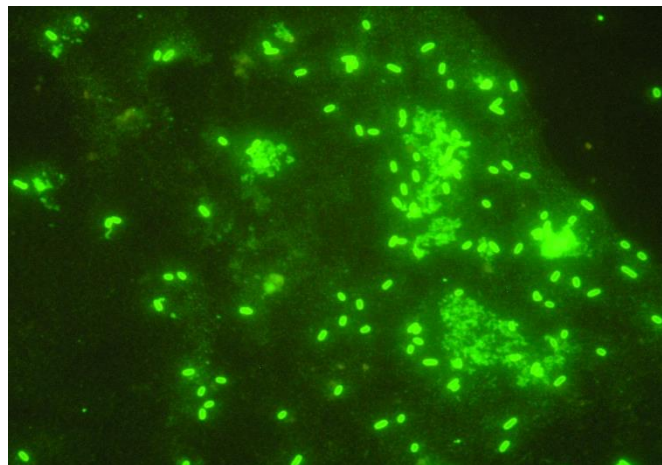
Figure, 8: Cell morphology of *R. solanacearum* under immunofluorescent (IF) microscope.

3. **Biovar determination of the pathogen**

    The biovars determination was based on the ability of isolates to produce acids from hexose and alcohol sugars. Data in Table (6) show that the thirty isolates were able to produce acids from lactose, maltose, and cellibiose. However, they were unable to produce acids from sorbitol, mannitol, and dulcitol denoting that, these thirty tested isolates were assigned to biovar 2. So, the dominant race in Egypt is race 3, biovar 2.

Table (6): Biovar determination of the selected isolates from different areas

Village	Isolate's number	Utilization of (Acid without gas)					
		Maltose	Lactose	Cellobiose	Mannitol	Sorbitol	Dulcitol
Abo Al Khawi	1	+	+	+	-	-	-
	2	+	+	+	-	-	-
	3	+	+	+	-	-	-
	4	+	+	+	-	-	-
	5	+	+	+	-	-	-
	6	+	+	+	-	-	-
	7	+	+	+	-	-	-
	8	+	+	+	-	-	-
	9	+	+	+	-	-	-
	10	+	+	+	-	-	-
	11	+	+	+	-	-	-
	12	+	+	+	-	-	-
Al Tayreya	13	+	+	+	-	-	-
	14	+	+	+	-	-	-
	15	+	+	+	-	-	-
	16	+	+	+	-	-	-
	17	+	+	+	-	-	-
	18	+	+	+	-	-	-
	19	+	+	+	-	-	-
	20	+	+	+	-	-	-
	21	+	+	+	-	-	-
Om Saber	22	+	+	+	-	-	-
	23	+	+	+	-	-	-
	24	+	+	+	-	-	-
	25	+	+	+	-	-	-
	26	+	+	+	-	-	-
	27	+	+	+	-	-	-
	28	+	+	+	-	-	-
	29	+	+	+	-	-	-
	30	+	+	+	-	-	-

4. **Pathogenic potentials of selected bacterial isolates**

Pathogenicity showed that all tested isolates representing different locations were able to wilt tomato seedlings 3 days after stem inoculation under greenhouse conditions.

5. **Real-time PCR (Taq-Man) assay**

Real-time PCR is a sensitive test for detection of low concentrations of *R. solanacearum* and is being considered a confirmatory test in the detection work. The RS primers and probe were employed to detect all biovars and races of *R. solanacearum*. Positive results were shown with all the tested isolates indicating that the thirty isolates were *R. solanacearum* (Figure., 9).

Figure**, 9**: Amplification of DNA extract of thirty selected isolates from different areas by Taq Man polymerase chain reaction (PCR). Negative and positive controls were included. The curves exceed the threshold considered positive.

6.   Phylotype assignment

Based on the results of the Pmx-PCR, all selected isolates belonged to the phylotype II sequevar I, as 372- bp amplicon was observed for the tested isolates (Figure,10: a,b and c) .
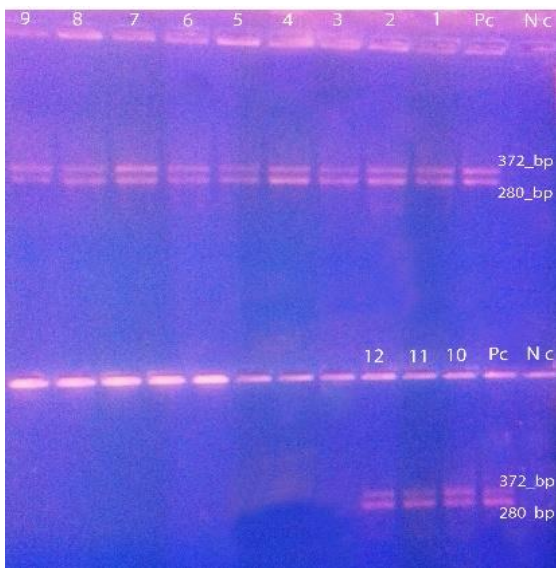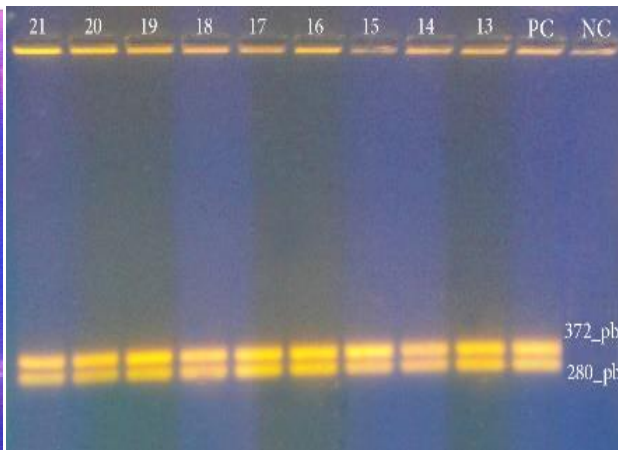
B(Al Tayreya area)

A(Abo Al Khawi area)
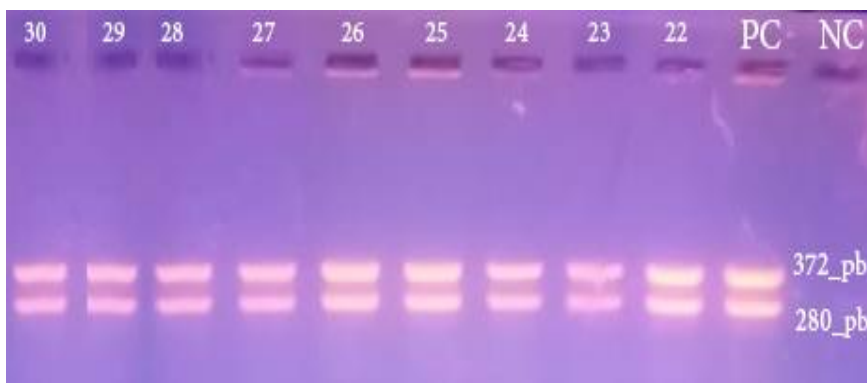
C (Om Saber area)
Figure, 10(a,b and c): PCR products of (30) isolate of *R. solanacearum* using different primers, 280-bp amplicon from *R.solanacearum* species and 372-bp amplicon from phylotype II strains.

II. Construction of soil and vegetation indices

1. Before planting indices construction

The results obtained from the application of the remote sensing technology over the infested locations before planting potato are shown in Table (7). The NDVI analysis showed near-zero values in the three field locations which reflects the absence of any kind of vegetation allowing for further analysis to the bare soil. The NDSI analysis for the involved soils showed positive values reflecting medium and relatively high soil salinity conditions. Both Al-Tayareya and Om Saber locations showed negative near-zero values in NDMI results, while, the soil at Abo El-Khawy location showed positive value which reflects relatively high moisture content at this location.

Table (7) : Pixel values resulted from the application of NDVI & NDSI over RapidEye images and NDMI which applied on Landsat 8 scene on bare soils before planting potato crop.

Location No.	Location Name	Latitude	Longitude	NDVI Value	NDMI Value	NDSI Value
1	Al-Tayareya	30°38'5.38"N	30°46'3.83"E	-0.02	-0.03	0.02
2	Abo El-Khawy	30°34'41.77"N	30°48'40.65"E	-0.02	0.2	0.02
3	Om Saber	0°31'43.56"N	30°47'29.74"E	0.01	-0.06	0.01

2. After planting indices construction

After applying both NDVI and MCARI analysis over the RapidEye images covering the study locations the results are shown in Table (8). The NDVI analysis showed positive values, around 0.30 reflecting that the fields at the three locations were planted. The chlorophyll contents of the potato leaves at all three locations reflected relatively medium contents contrary to what was assumed at this growth stage of high levels of chlorophyll to reach values above 0.8 in the thematic data resulted from MCARI.

Table 8: Pixel values resulted from the application of NDVI and MCARI over RapidEye images during medium growth stages of the potato crop.

Location No.	Location Name	Latitude	Longitude	NDVI Value	MCARI Value
1	Al-Tayareya	30°38'5.38"N	30°46'3.83"E	0.38	0.63
2	Abo El-Khawy	30°34'41.77"N	30°48'40.65"E	0.38	0.58
3	Om Saber	0°31'43.56"N	30°47'29.74"E	0.31	0.58

Based on the analyses made on the soils (both in the field and isolated samples) and foliage of plants using both lab tests and remote sensing analyses, the effects of bacterial infections with *R. solanacearum* can be monitored continuously over vast areas of fields planted with potato crops to detect any reduction in the chlorophyll levels in the leaves which may be caused by such bacterium type or any other disease that may cause an uncharacteristic decrease in chlorophyll contents.

Discussion

Bacterial wilt of potato caused by *R. solanacearum* (Syn. *P. solanacearum*) is the most serious bacterial disease predominating in warm and temperate potato districts at certain conditions (Yabuuchi *et al*., 1995). This disease has causes a lot of quarantine problems for Egyption potato exportation since the first report made by Sabet (1961) and has been studied intensively by Farag(1970) and (1976). The bacterium is classified as tuber-borne disease, in principal, with extended longivity in infested fields that complicate agriculture practices for control, along with possible occurence of susceptible and multiple weed flora (unpublished data). The bacterium has more than 4 races at the time being with predominance of "Race 3" at certain old potato cultivation district in Egypt. No evidence is being made of the occurence of the most serious and hazardous race 1 bacteria in Egypt. The disease produced by race 3 has been surveyed in Egypt by Michail *et al*. (1974) by the classical methods of diagnosis and diseased areas were coded and prohibited from potato exportation.

Because of complexity of field work during the survey and extended planting potatoes, more accurate and rapid screening methods were followed. Among these modern and advanced methods of detection is to follow the analyses of the occurence of the disease through remote sensing (Nilsson, 1995 and Chavez *et al*., 2012).

In the present work, isolation of the pathogen was made from naturally infested soil(s) from previously enlisted potato cultivation districts in three villages (Aboelkhawy, Tayareya, Omsaber) at Behera governorate (North of Nile delta). Several investigators reported occurrence of potato brown rot bacteria in other location of Egypt (Hamad *et al*., 2008 & 2016; Hassan *et al*., 2017 and Hanafy *et al*., 2018). Methods currently used for the detection of *R. solanacearum* through plating on modified semi-selective medium (Elphinstone *et al*., 1996) and immunofluorescent antibody staining (Janse, 1988). Complimentary procedures including a tomato bioassay (Janse, 1988), real-time PCR assays (Weller *et al*., 2000) and Phylotype assignment (Sagar *et al*., 2014). Many researchers clarified that these methods differ in their degree of sensitivity (Mikhail, *et al*., 2016). Plating technique on modified (SMSA) medium is a microbiological selective method although some samples may show saprophytic bacteria (Pradhanang *et al*., 2000). It may requires skilled and well trained personnel who can distinguish target colonies from other saprophytes that can grow on the medium. Immunofluorescent antibody staining (IFAS) is a serological technique and considerd one of the first standard screening tests for detecting latent infection of *R. solanacearum* in potato tubers. This method with the polyclonal antisera was described as a rapid and inexpensive method but lack in sensitivity beside giving a false positive results due to cross-reactions with other bacteria (Balabel, 2014). Using tomato seedling as biological test was reliable to detect as few as 10^4 cells / mL (Janse, 1988 and Elphinstone *et al*., 1996). Tomato seedlings are showing wilt symptoms within a week from inoculation depending on the starting inoculum (inoculum potential) and optimization of conditions (Elphinstone *et al*., 1996), however, if temperature falls below 21ºC the infection takes place but no symptoms could be recognized i.e, the wilt may fail to develop (Singh *et al*., 2014). The results of biovar determination indicating that all the tested isolates belong to biovar 2. On the other hand, phylotype specific multiplex (Pmx)- PCR revealed that all thirty isolates of *R. solanacearum* belonged to phylotype II as a 372- bp amplicon was observed for all the tested isolates after electrophoresis (Agarose gel 2% w/v). These results indicating that, the race 3, biovar 2 (phylotype II, sequevar I) is dominant race in Egypt, the same results were observed by other searchers (Hamad *et al*., 2016; Hassan, *et al*., 2017).

Remote sensing technology was applied in this research by using satellite images from Landsat 8 and RapidEye before planting (bare soil conditions) and after planting. Soil salinity, soil moisture, and plant chlorophyll content were checked over the acquired satellite images

through the application of Normalized Difference Moisture Index (NDMI), Normalized Difference Vegetation Index (NDVI), Normalized Difference Salinity Index (NDSI) and Modified Chlorophyll Absorption Ratio Index (MCARI) indices. It is known that at early stages of bacterial infection, the first recognized symptoms developed on the plant leaves as wilting of young leaves followed by general wilting and yellowing of the leaves and finally plant death (Champoiseau & Momol, 2009)

Results of remote sensing analysis revealed chlorophyll levels were in medium levels which was not typical to conditions associated with usual conditions. Moreover, analyses showed medium or relatively high salinity along with high moisture content. The latter two factors might be involved in disease progress, as shown by chlorophyll level change. It is known that, the capability of remotely sensing light reflectance to detect the damage caused by bacteria is depending on changes in reflectance introduced approximately by the blockage of vascular tissue of the infected plants (Grimault *et al*. 1994; Herna´ndez *et al.* 2005). Any stress on the plant leads to different physiological and morphological changes in affected plants and remote sensing technique can detect early morphological and anatomical changes even if these changes are small (Cha´vez *et al*. 2009, 2010). Moreover, Cha´vez *et al*., (2012) noted that different plant reactions, caused by different factors (e.g. bacteria, virus, water deficits, meterological aspects) may be well detected by test sensing devices and analytical ways. Also, Mahlien, 2016 used different imaging sensors to detect different plant diseases.

Therefore, the results of processing of satellite images denoting unusual growth conditions that may be attributed to disease progress. Such an approach can be applied by decision-makers as precautionary aspects to rapid and presumptive surveys of disease incidence of vast areas cultivated with potato crops and /or any other crop. Also, it could help farmers and producers to be more focalized and timely response to intra-field and intra-crop variations such as the outbreak of disease. For clarification , remote sensing has been used to detect many diseases that affect plants, for example: phytophthora foot rot in citrus trees (Fletcher *et al*.,2001) ;late blight in tomatoes (Zhang *et al*.,2005); yellow rust in wheat (Huang *et al*.,2007); citrus greening disease (Kumar *et al*.,2012); downy mildew in cucumber (Tian and Zhang,2012) ; powdery mildew in winter wheat (Yuan *et al*.,2014) ; grapevine leafroll disease - GLD (MacDonald,2016); yellow leaf curl disease in tomato leaves (Lu et al.,2018) and fusarium wilt in Banana (Ye *et al*.,2020).

It is very important to note that successful use of remote sensing depends on the accurate study of healthy and diseased plants. Otherwise we must compare and analyze remote sensing data

from healthy plants with data from plants under stress. In this point, Lowe *et al.*, 2017 used the imaging techniques to detect biotic and abiotic stress in plants. However, further work is advised to explore the validity of remote sensing of plant diseases at larger scale to help in disease control.

Acknowledgment

References

Aldakheel, Y. Y., Elprince, A. M., & Al-Hosaini, A. I. (2005). Mapping of salt-affected soils of irrigated lands in arid regions using remote sensing and GIS. RAST 2005 - Proceedings of 2nd. International Conference on Recent Advances in Space Technologies, 2005, 467–472. https://doi.org/10.1109/RAST.2005.1512614.

Balabel, N.M. (2014). Species Determination of Cross-Reacting Bacteria in Immuno-fluorescens Diagnosis of Potato Brown Rot. Plant Pathology Journal, 13 (1):28-36.

Buddenhagen, I., & Kelman, A. (1964). Biological and Physiological Aspects of Bacterial Wilt Caused by *Pseudomonas solanacearum.* Annual Review of Phytopathology, 2(1): 203–230. https://doi.org/10.1146/annurev.py.02.090164.001223.

Caitilyn, A., Philippe, P., and Hayward, A.C. (2005). Bacterial wilt disease and the *Ralstonia solanacearum* species complex. APS Press, St Paul, MN, USA. http://publications.cirad.fr/une_notice.php?dk=524964.

Cha´vez, P., Yarleque´, C., Piro, O., Posadas, A., Mares, V. , Loayza, H., Carlos,C., Zorogastua, P., Flexas,J. and Roberto, Q. (2010). Applying multifractal analysis to remotely sensed data for assessing PYVV infection in potato (*Solanum tuberosum* L.) crops. Remote Sensing Journal, 2(5): 1197-216.

Cha´vez, P. , Yarleque´, C., Loayza,H., Mares,V., Hancco,P., Priou,S. and Pilar, M., Posadas,A., Zorogastu´a, p., Flexas, J.and Roberto, Q. (2012). Detection of bacterial wilt infection caused by *Ralstonia solanacearum* in potato (*Solanum tuberosum* L.) through multifractal analysis applied to remotely sensed data. Precision Agric., 13:236-255. DOI 10.1007/s11119-011-9242-5.

Cha´vez, P., Zorogastu´a, P., Chuquillanqui, C., Salazar, L. F., Mares, V., and Roberto, Q. (2009). Assessing Potato Yellow Vein Virus (PYVV) infection using remotely sensed data. International Journal of Pest Management, 55: 251-256.

Chiwaki, K., Nagamori, S., and Inoue, Y. (2005). Predicting bacterial wilt disease of tomato plants using remotely sensed thermal imagery. Journal of Agricultural Meteorology, 61: 153-164.

Champoiseau, P. G., and Momol, T. M. (2009). Bacterial wilt of tomato. The United States

Department of Agriculture - National Research Initiative Program (2007-2010). https://plantpath.ifas.ufl.edu/rsol/Trainingmodules/BWTomato_Module.html.

Economic Affairs Sector (E.A.S.). Ministry of Agriculture and Land Reclamation (2018). Bulletin of the Agricultural Statistics, Part(2), Summer & Nili Crops 2016/2017.

Egyptian Ministry of Environment, (2007). Environmental Description of El Beheira Government.

Elphinstone, J. G., Hennessy, J., Wilson, J. K., and Stead, D. E. (1996). Sensitivity of different methods for the detection of *Ralstonia solanacearum* in potato tuber extracts. EPPO Bulletin, 26(3- 4): 663-678. (https://doi.org/10.1111/j.1365-338.1996.tb01511.x).

Ennaji, W., Barakat, A., Karaoui, I., El Baghdadi, M., and Arioua, A. (2018). Remote sensing approach to assess salt-affected soils in the north-east part of Tadla plain, Morocco. Geology, Ecology, and Landscapes, 2(1): 22-28. https://doi.org/10.1080/24749508.2018.1438744

Farag, N.S. (1970). Studies on Brown Rot of Potato in Egypt (M.Sc.) Department of Microbiology, Fac. of Agric., Ain Shams Univ..

Farag, N.S. (1976). Interaction Between Some Soil Microflora and *Pseudomonas solanasearum* (Ph.D). Department of Microbiology, Fac. of Agric., Ain Shams Univ.

Fletcher, R. S., Skaria, M., Escobar, D. E. Everitt, J. H. (2001). Field spectra and airborne digital imagery for detecting phytophthora foot rot infections in citrus trees. Hort Science, 36(1): 94 – 97.

Grimault, V., Gelie, B., Lemattre, M., Prior, P., and Schmit, J. (1994). Comparative histology of resistant and susceptible tomato cultivars infected by *Pseudomonas solanacearum.* Physiological and Molecular Plant Pathology, 44: 105-123.

Habashy, W. H. S., Fawzi, F. G., El-Huseiny, T. M., and Neweigy, N. A. (1993). Bacterial wilt of potatoes. II. Sensitivity of the pathogen to antibiotics and pathogenesis by streptomycin-resistant mutants. Egyptian Journal of Agricultural Research, 71: 401-412.

Hanafy, M.S., El-Habbaa, G.M., Mohamed, F.G. , Balabel, N.M. and Ahmed, G.A. (2018). Surveying and Fast Detection of *Ralstonia solanacearum* Bacterium in Some Egyptian governorates. Annals of Agric. Sci., Moshtohor, 56(2): 405- 416. ISSN: 1110- 0419.

Hamad, Y.I., Tohamy, M.R. and El-Morsy, G.A. (2008). Detection of *Ralstonia solanacearum* on som crops and weeds under Egyption conditions. Zagazig J. Agric. Res., 35 (4): 769-788.

Hamad, Y.I., Youssef, S.A, Balabel N.M., Shaaban W. I. and Ahmed, M.I. (2016). Detection the causal organism of potato brown rot bacterium in potato and water canals. Egypt . J. of Appl. Sci., 31(6):90-109.

Hassan, E.A., Balabel N.M., Ahmed A.E., Eid, N.A. and Ramadan, E .M. (2017). Relationship between *Ralstonia solanacearum* and bio-agents recovered from different habitats.

International Journal of Scientific & Engineering Research, 8, (1):91-104. ISSN 2229-5518.

Hayward, A.C. (1964). Characteristics of *Pseudomonas solanacearum.* Journal of Applied Bacteriology, 27(2): 265-277. https://doi.org/10.1111/j.1365-2672.1964.tb04912.x

Hayward, A.C. (1991). Biology and epidemiology of bacterial wilt caused by *Pseudomonas solanacearum.* Annual Review of Phytopathology, 29(1): 65-87. https://doi.org/10.1146/annurev.py.29.090191.000433

Hayward, A.C., and Hartman, G.L. (1994). Bacterial wilt: the disease and its causative agent, *Pseudomonas solanacearum.* CAB International, Wallingford.

Herna´ndez, Y., Marino, N., Trujillo, G., and Urbina de Navarro, C. (2005). Invasio´n de *Ralstonia solanacearum.* en tejidos de tallos de tomate (*Lycopersicon esculentum Mill). Revista de la Facultad de* Agronomı´a, 22(2): 181-190.

Huang, W., Lamb, D.W., Niu, Z., Zhang, Y., Liu, L. and Wang, J. (2007). Identification of yellow rust in wheat using in-situ spectral reflectance measurements and airborne hyperspectral imaging. Precision Agric., 8:187–197. DOI 10.1007/s11119-007-9038-9

Janse, J.D. (1988). A detection method for *Pseudomonas solanacearum* in symptomless potato tubers and some data on its sensitivity and specificity. EPPO Bulletin, 18(3): 343-351. https://doi.org/10.1111/j.1365-2338.1988.tb00385.x

Ji, P., Momol, M.T., Olson, S.M., Hong, J., Pradhanang, P., Anith, K.N., and Jones, J.B. (2005). New tactics for bacterial wilt management on tomatoes in the Southern U.S. Acta Horticulturae, 695:153-159. https://doi.org/10.17660/actahortic.2005.695.17

Kabeil, S.S., Lashin, S.M., El-Masry, M.H., El-Saadani, M.A., Abd-Elgawad, M.M., and Aboul-Einean, A.M. (2008). Potato brown rot disease in Egypt: Current status and prospects. J. Agric. & Environ. Sci., 4(1): 44-54.

Kelman, A. (1953). The bacterial wilt caused by *Pseudomonas solanacearum* : a literature review and bibliography. North Carolina Agricultural Experiment Station.

Kelman, A. (1954). The relationship or pathogenicity in *Pseudomonas solanacearum* to colony appearance on a tetrazolium medium. Phytopathology, 44(19): 693-695.

Kumar, A., Lee, W.S. , Ehsani, R.J., Albrigo L.G. , Yang, C. and Mangan ,R.L.(2012). Citrus greening disease detection using aerial hyperspectral and multispectral imaging techniques. Journal of Applied Remote Sensing 6(1):063542.1-22.

Lo´pez, M.M., and Biosca, E.G. (2004). Potato bacterial wilt management: New prospects for an old problem. In C. Allen, P. Prior, & A. C. Hayward (Eds.), Bacterial wilt disease and the *Ralstonia* species complex (pp. 205–224). St. Paul, MN: APS Press.

Lowe, A., Harrison, N. and French, A.P. (2017). Hyperspectral image analysis techniques for the detection and classification of the early onset of plant disease and stress. Plant Methods, 13:80, DOI 10.1186/s13007-017-0233-z

Lu, J., Zhou, M., Gao, Y. and Jiang, H. (2018). Using hyperspectral imaging to discriminate yellow leaf curl disease in tomato leaves. Precision Argic., 19:379 –394. https://doi.org/10.1007/s11119-017-9524-7

Macdonald, S.L., Staid, M., Staid, M. and Cooper, M.L. (2016). Remote hyperspectral imaging of grapevine leaf roll-associated virus 3 in cabernet sauvignon vineyards. Computers and Electronics in Agriculture, 130: 109 -117. DOI: 10.1016/j.compag.2016.10.003

Mahlien, A.K.(2016). Plant disease detection by imaging sensors- parallels and specific demands for precision agriculture and plant phenotyping. Plant Disease, 100 (2): 241 - 251.

Mikhail, M.S., Abdel-Alim, A.I., Gebreal, F. and Ali E.E. (2016). Comparison between different methods for detection of *Ralstonia solanacearum* in soil. J. Biol. Chem. Environ. Sci., 11 (4): 333-349.

Mickail, M.Y.; Bishay, F.; Farag ,N.S. and Tawfik, A.E. (1974). Evaluation of bacterial wilt disease in A.R.E. during the years from 1967-1968 to 1971-1972. Agric. Res. Rev., Cairo, 52: 89-94.

Murakoshi, S., and Takahashi, M. (1984). Trials of some control of tomato wilt caused by *Pseudomonas solanacearum*. Bulletin of the Kanagawa Horticultural Experiment Station, 31: 50-56.

Nilsson, H.E.(1995). Remote sensing and image analysis in plant pathology. Annu. Rev. Phytopathol., 33:489-528.

OEPP/EPPO (Organisation Europeenne pour la Protection des Plantes / European Plant Protection Organization), 1990. Quarantine procedures no., 26.*Pseudomonas solanacearum.*OEPP/EPPO Bulletin, 20:255-262.

Opina, N.F., Tavner, G., Halloway, J.F., Wang, T.H.L.R, Maghirang, M., Fegan, A.C, Hayward, V., Krishnapillai, W.F., Hong, B.W. and Holloway, J.N. (1997). A novel method for development of species and strain - specific DNA probes and PCR primers for identifying *Burkholderia solanacearum* (formerly *Ps. solanacearum*). As.Pac.J.Mol. Biol. Biotechnol., 5:19-33

Planet Labs. (2016). Rapideye^{TM} Imagery Product Specifications (Issue Version 6.1).

Pradhanang, P.M., Elphinstone J.G. and Fox, R.T. (2000). Identification of crop and weed hosts of *R. solanacearum* biovar 2 in the hills of Nepal. Plant Pathology, 49: 403-413.

Roy, D.P., Wulder, M.A., Loveland, T. R., C.E., W., Allen, R.G., Anderson, M.C., Helder, D., Irons, J. R., Johnson, D. M., Kennedy, R., Scambos, T.A., Schaaf, C.B., Schott, J. R., Sheng, Y., Vermote, E.F., Belward, A.S., Bindschadler, R., Cohen, W.B., Gao, F. and Zhu, Z. (2014). Landsat-8: Science and product vision for terrestrial global change research. Remote Sensing of Environment, 145: 154-172. https://doi.org/10.1016/j.rse.2014.02.001

Sabet, K.A. (1961). The occurrence of bacterial wilt of potatoes caused by *Pseudomonas solanacearum* (E.F. Smith) in Egypt. Min. of Agric., Extension Dept., Tech. Bull., 112: 116-119.

Saddler, G.S. (2005). Management of bacterial wilt disease. In: Bacterial wilt disease and the

Ralstonia solanacearum species complex. C.Allen, P. Prior and A.C. Hayward (eds.). *American Phytopatholocial Society*, St. Paul MN.

Sagar,V.,Gurjar, M.S., Jeevalatha, A., Bakade, R.R., Chakrabarti, S.K., Arora, R.K. and Sharma S. (2014). Phylotype analysis of *Ralstonia solanacearum* strains causing potato bacterial wilt in Karnataka in India. Afr. J. of Microbiol. Res., 8(12):1277-1281.

Serrano, J., Shahidian, S., and da Silva, J.M. (2019). Evaluation of normalized difference water index as a tool for monitoring pasture seasonal and inter-annual variability in a Mediterranean agro-silvo-pastoral system. Water (Switzerland), 11(1): 20. https://doi.org/10.3390/w11010062

Singh, D., Yadav, D.K., Sinha, S. & Choudhary, G. (2014). Effect of temperature, cultivars, injury of root and inoculums load of *Ralstonia solanacearum* to cause bacterial wilt of tomato. Arch. of Phytopathol. and Plant Protec., 47(13):1574 -1583.

Tian, Y. and Zhang, L.(2012). Study on the methods of detecting cucumber *Downy mildew* using hyperspectral imaging technology. International Conference on Medical Physics and Biomedical Engineering, Physics Procedia, 33: 743 – 750.

Warner, T.A., Nellis, M.D., and Foody, G.M. (2009). The SAGE Handbook of Remote Sensing. In The SAGE Handbook of Remote Sensing. https://doi.org/10.4135/9780857021052

Weier, J., and Herring, D. (2018). Measuring Vegetation (NDVI & EVI) : Feature Articles. 2000. https://doi.org/10.1111/j.1365-246X.2011.05323.x

Weller, S.A., Elphinstone, J.G., Smith, N.C., Boonham, N., and Stead, D.E. (2000). Detection of *Ralstonia solanacearum* strains with a quantitative, multiplex, real-time, fluorogenic PCR (TaqMan) assay. Applied and Environmental Microbiology, 66(7):2853-2858. https://doi.org/10.1128/AEM.66.7.2853-2858.2000

Xue, J., and Su, B. (2017). Significant remote sensing vegetation indices: A review of developments and applications. Journal of Sensors, 2017: 1-17. https://doi.org/10.1155/2017/1353691

Yabuuchi, E., Kosaka, Y., Yano, I., Hotta, H. and Nishiuchi,Y. (1995). Transfer of two *Burkholderia* and *Alcaligenes* species. To *Ralstonia* gen. nov.; Proposal of *Ralstonia picketii* (Ralston, Palleroni and Doudoroff 1973) Comb. nov.; *Ralstonia solanacearum* (Smith, 1896) Comb. nov. and *Ralstonia eutropha* (Davis 1969) Comb. nov. Microbial. Immunol., 39 (11): 897-904.

Ye, H., Huang, W., Huang, S., Cui, B., Dong, Y., Guo, A., Ren, Y. and Jin, Y. (2020). Recognition of banana fusarium wilt based on UAV remote sensing. Remote Sens, 12 (938):2-14.

Yuan, L., Zhang, J., Shi, Y., Nie, C., Wei, L. and Wang, J. (2014). Damage Mapping of Powdery Mildew in Winter Wheat with High-Resolution Satellite Image. Remote Sens., 6: 3611-3623; doi: 10.3390/rs6053611

Zhang, M., Qin, Z., and Liu, X.(2005). Remote sensed spectral imagery to detect late blight in field tomatoes. Precision Agriculture, 6: 489–508.

فعالية التقنيات المعتمدة على تفاعل البلمرة المتسلسل وتكنولوجيا الاستشعار من البعد فى الكشف عن بكتريا ال *R. solanacearum* المسببة لاصابة البطاطس بالعفن البنى

نجلاء موسى بلابل[1,2]ـ ممدوح محمد على[3] ـ شمس نورالدين يونس [4]

[1] معهد بحوث آمراض النباتات ـ مركز البحوث الزراعية ـ الجيزة ـ مصر

[2] مشروع حصر ومكافحة مرض العفن البنى فى البطاطس ـ دقى ـ الجيزة ـ مصر

[3] قسم الجيولوجيا ـ كلية العلوم ـ جامعة الازهر ـ مدينة نصر ـ مصر

[4] قسم الجغرافيا ـ كلية الاداب ـ جامعة القاهرة ـ الجيزة ـ مصر

يعتبر مرض الذبول البكتيرى الناتج عن بكتيريا *Ralstonia solanacearum* phylotype II (2 biovar 3 race) sequevar I واحد من أخطر الامراض البكتيرية للبطاطس. هدفت هذه الدراسة الى الكشف عن التدهور الناتج عن هذه البكتيريا من خلال تسجيل بيانات الاستشعار من البعد. لهذا الغرض تم أختيار بعض المناطق المصابة طبيعيا فى بعض القرى التابعة لمحافظة البحيرة وهى :
أبو الخاوى ، الطيرية وأم صابر لعزل بكتيريا ال*Ralstonia solanacearum* . تم انتقاء ثلاثون عزلة عشوائيا من البيئة شبه الانتقائية (SMSA medium) وتم اختبارهم بعد ذلك بواسطة أختبار الوميض الفلورسنتى (IFAS) وتم التأكيد عليهم بأستخدم الاختبار الحيوى عن طريق حقن نباتات الطماطم صنف (Pinto) وكانت النتائج ايجابية . أعطت كل العزلات المختبرة نتائج ايجابية مع أختبار-Real-Time PCR). كما اشارت النتائج على ان كل عزلات بكتيريا ال *Ralstonia solanacearum* تابعة لـ phylotype II بناءا على نتائج PCR –(Pmx) Phylotype Specific Multiplex حيث تلاحظ وجود بندات الحمض النووى (amplicon DNA) عند 372pb.

تم تطبيق المؤشرات الطيفية بأستخدام صور الاقمار الصناعية (Landsat 8 and RapidEye) وشملت هذه المؤشرات الغطاء النباتي المعياري (NDVI) ، مؤشر ملوحة التربة (NDSI) ، مؤشر الرطوبة المعياري (NDMI) ومؤشر معدل امتصاص الكلوروفيل المعدل (MCARI). أظهرت نتائج تحاليل الاستشعار من البعد ان ملوحة التربة ومحتواها الرطوبي من متوسط إلى مرتفع نسبيًا ، علاوة الى ذلك فأن مستويات الكلوروفيل في النباتات كانت في مستويات متوسطة وليست بالمستوى الطبيعى للنباتات السليمة فى الظروف المعتادة. تحتاج هذه الدراسة إلى مزيد من البحث والتطبيق على الاراضى المصابة .